

Discussion of Lean Modelling Approaches for Powertrains of Combine Harvesters

Fabian Wohlfahrt, Thomas Göres, Stefan Terörde, Ludger Frerichs

Modelling powertrains on modern combine harvesters can become a task of enhanced complexity. The polymorphic form and branched design of both mechanical and hydraulic transmission parts make recording and modelling single power flows a significant effort. To find a practical way for modelling of principal loads on an existing machine, this paper therefore presents an alternative approach. The goal is to reduce efforts regarding measurement equipment as well as data analysis in the following modelling process. By introducing conceptual guidelines for lean modelling, an approach is presented that allows a simplified modelling of loads on powertrains of modern combine harvesting machinery. By utilizing it on exemplary machine data its potential and possible use cases are discussed.

Keywords

Combine harvester, load modelling, measurement, powertrain

Measuring occurring loads on powertrains of combine harvesting machinery is a difficult task. A combine harvester executes a set of adjacent agrotechnical processes that require a significant amount of power. The main consumers are the functional technology (header, threshing system, separation, cleaning, chopping unit), the (mostly hydrostatic) ground drive, as well as significant auxiliary consumers, e.g., engine fan, (MEINERS und BÖTTINGER 2018, HÄBERLE 2019, MEINERS 2023). Common modelling approaches for this purpose are source-based measurement concepts. These record the loads of these aggregates separately divided by their functions. Different source-based measurement campaigns for combine harvesters are known in the literature (MÜLLER et al. 2012, FILLINGHAM 2017, HÄBERLE 2019, MEINERS 2023) and give valuable information about the load characteristics of the single aggregates. The presented approaches focus on stationary correlation to the throughput and create a convenient knowledge base for the principal power flow in a combine powertrain.

Implementing the necessary measurement devices can quickly become an extensive task. Strain-gauge based torque measurement devices need to be integrated on the entire powertrain. This creates constructive challenges to find sufficient integration space for the measurement devices. Partly, their integration even changes the construction of central parts significantly. This may conflict with the validation of the original component. Measuring hydraulic loads can be executed comparatively more easily because the equipment can be integrated in pipes and connectors. However, this introduces additional (partly cost-intensive) equipment into the system. Furthermore, this leads to connected system changes and installation effort. In consequence only a small set of machinery can be analysed.

Besides the aspects regarding measurement, the factor of modelling and parametrizing virtual systems afterward can become time-consuming. Source-based approaches require to model all powertrain branches in their entirety. This is necessary, if single power flows need to be analysed. If, however, the overall behavior of the machine is in focus of analysis, this is not a must-have. Recognizing those

points reveals several aspects that hinder an exhaustive utilization of source-based measurement and modelling approaches for development tasks of combine harvesting machinery.

Therefore, the introduction of simplified modelling approaches can become of particular interest for tasks where the split of power flows is of lower significance. While analysing defined parts of the functional apparatus (e.g. the threshing system) requires separate measurement equipment, a variety of measurement and validation tasks does not. For evaluating machine systems as a whole, as well as for the modelling of loads on central parts of the powertrain a detailed representation of the single branches of a powertrain is not necessary. The main interest here lies more in the modelling of main characteristics regarding power-influence and dynamics on machines, which are as close as possible to the final production machines.

To achieve the introduced goals, principal concepts for lean modelling are introduced as a potential design guideline to reduce measurement and modelling efforts. Subsequently, model representations for a modern powertrain structure based on a combine of the type Claas Lexion are presented. This creates a groundwork for a discussion of the required efforts, achievable model quality, and possible use cases.

Motivation for lean modelling approaches

The basic idea of the targeted lean modelling approach is the allocation of certain power flows of a measured load to a defined origin without necessarily measuring them directly. This requires a certain understanding of the system to be measured. Therefore, principal pre-assessments of these sources, which can be achieved by prior measurement or through empirical knowledge, are needed. A popular example of this concept are driving resistance formulas, which are used in practical automotive development and evaluation tasks. Equation 1 describes the loads occurring on a vehicle driving on a road – the driving resistance formula according to KÜÇÜKAY (2022). Here, rolling resistance, an aerodynamically induced counterforce, and slope-induced effects are assumed. These sum up to a collective of forces, which act on the car and cause a change of its velocity, following Newton's first law.

$$m \cdot a = F_{Roll} + F_{Air} + F_{Slope} + F_{Driving} \quad (\text{Eq. 1})$$

with:

m : Vehicle mass
 a : Acceleration

F_{Roll} : Rolling resistance
 F_{Air} : Air resistance

F_{Slope} : Incline resistance
 $F_{Driving}$: Driving force

Determining those forces in a source-based manner would require a set of measurements. Each wheel would need to be equipped with torque measurement devices and the vehicle would need to be placed in a wind channel to measure wind resistance effects. Though both measures are common and suitable for optimizing single components, lean approaches are used to gain information for modelling in a much simpler way. In coast-down experiments, the tested vehicle is simply decelerated by the acting forces from a defined starting point at a certain speed. By measuring the vehicle weight beforehand and recording the vehicle speed, the coast-down curve can be fitted allocating the acting deceleration forces to single effects by regression. Equation 2 shows a regression formula with (simplified) constant rolling resistance factors and an assumed air resistance with a quadratic correlation to vehicle speed, according to KÜÇÜKAY (2022). Neither the forces nor their distribution are measured

directly. Still, a practical modelling of the driving resistance can be achieved, which can serve in later development purposes, e.g., on test benches (SCHWEHN et al. 2021, KÜÇÜKAY 2022).

$$m \cdot a = m \cdot f_r \cdot g \cdot \cos(\alpha) + \frac{1}{2} \cdot \rho_{Air} \cdot c_w \cdot A \cdot v^2 + m \cdot g \cdot \sin(\alpha) \quad (\text{Eq. 2})$$

with:

| | | |
|-----------------------------------|-------------------------------|------------------------|
| m : Vehicle mass | ρ_{Air} : Air density | v : Vehicle speed |
| a : Acceleration | A : Cross-section | α : Slope angle |
| f_r : Rolling resistance factor | c_w : Air resistance factor | g : Gravity constant |

The goal of the presented approach is to formulate an comparable approach to describe the power flows on a combine. The approach divides the acting forces and torques into three general sources: Base loads define the amount of power needed to operate the machine without moving or processing crops. Especially with main drives engaged, this represents a significant part of engine power capacity. Traction-induced loads occur from the driving resistance of the machinery as it accelerates, overcomes rolling resistance, and climbs possible slopes. The process-induced load describes occurring loads correlated with the throughput. Equation 3 shows the power sources of the approach:

$$\Sigma P = P_{Base} + P_{Traction} + P_{Process} \quad (\text{Eq. 3})$$

with:

| | | |
|------------------------|--|--------------------------------------|
| P_{Base} : Base Load | $P_{Traction}$: Traction-induced load | $P_{Process}$: Process-induced load |
|------------------------|--|--------------------------------------|

Therefore, predominantly linear correlations between throughput and power as well as between vehicle speed and power (and thus between vehicle speed and throughput) are assumed. To illustrate this load distribution and its general validity, a source-based collective according to HÄBERLE (2019) is used for comparison (Figure 1). Häberle used strain-gauge-based torque-measurement devices, hydraulic measurements, J1939-data, and model-based approaches. Corresponding data can be found e.g. by MEINERS (2023). Häberle identified mainly linear correlations between throughput and the power distribution of central parts of the functional technology (e.g. threshing unit, chopper unit, and separator), as well as significant parts of base loads occurring independently of the measured throughput as constant loads. Through the mainly linear character, a principal superposability can be assumed. This allows to aggregate different load groups to the distribution from Equation 3. Figure 2 shows the presented distribution based on the dataset from Häberle. Using process knowledge about the main dependencies of load sources from power-source-based measurements, a significant aggregation of single load groups can be performed. This significantly reduces the effort required to model machine behaviour under specific machine configurations and field conditions. This concept allows for a measurement consisting of data sources already available on standard machines (throughput measurement, engine torque, data from the hydraulic driveline). The goal is to depict the machine characteristics in terms of required power and dynamic behaviour, allowing to create a load model representation of a combine application. In the subsequent part a measurement concept is introduced on the base of measurements on a standard machine of the type Claas Lexion. Utilizing a set of exemplary measurement data, the validity of the approach is then discussed.

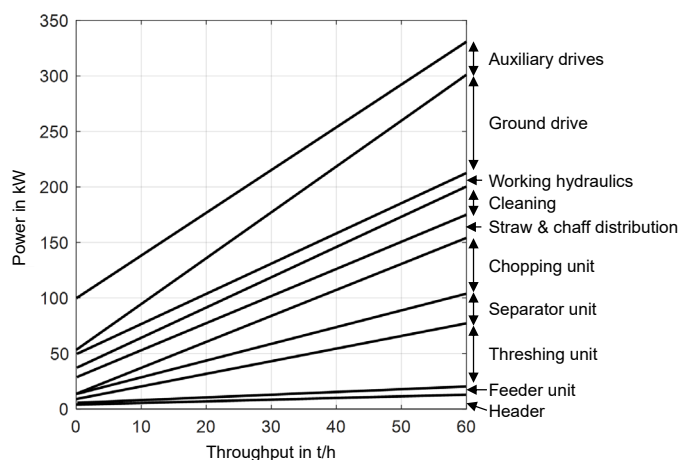


Figure 1: Source-based measurement of power distribution for a hybrid combine harvester, data according to HÄBERLE (2019)

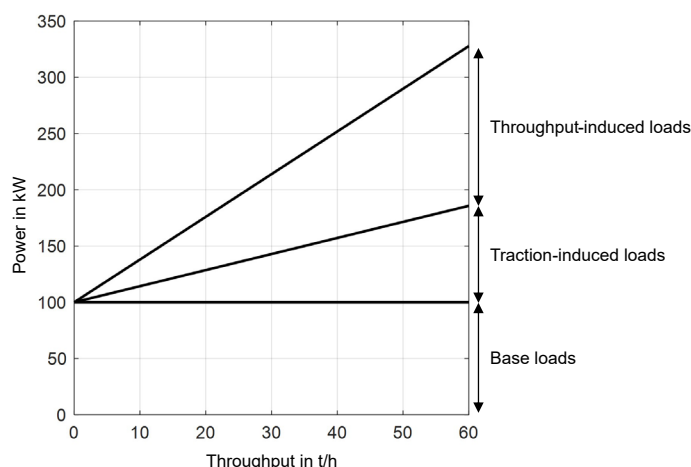


Figure 2: Lean form of combine loads, data according to HÄBERLE (2019)

Material and Methods

The goal of the measurement campaign is to measure all occurring forms of loads by using data sources available on a standard machine without any additional measurement equipment. As a technological basis, combines of the type CLAAS LEXION are chosen. In the exemplary data LEXION machines of the 8000 series are utilized. Using a modern diesel engine equipped with electronic OBD systems based on the CAN-J1939 standard, central data of the power unit (torque, engine speed, fuel consumption) can be obtained from the engine. As shown via testbench measurements, these data sources can be used and post-processed to serve as an eligible source of general torque information (ROHRER et al. 2018, WOHLFAHRT et al. 2024). The ground drive system is operated by electronically actuated hydrostatic units. Therefore, information about the power flows of the ground drive system can be deduced by utilizing data on the unit displacements, speeds, and differential pressures. Furthermore, speeds of central aggregates of the functional technology (e.g., threshing drum, rotor, cleaning fan) as well as of central auxiliary consumers (e.g. the cooling fan) are available. Figure 3 shows a simplified scheme of

a combine powertrain and the available data sources for the determination of power flows and rotating speeds.

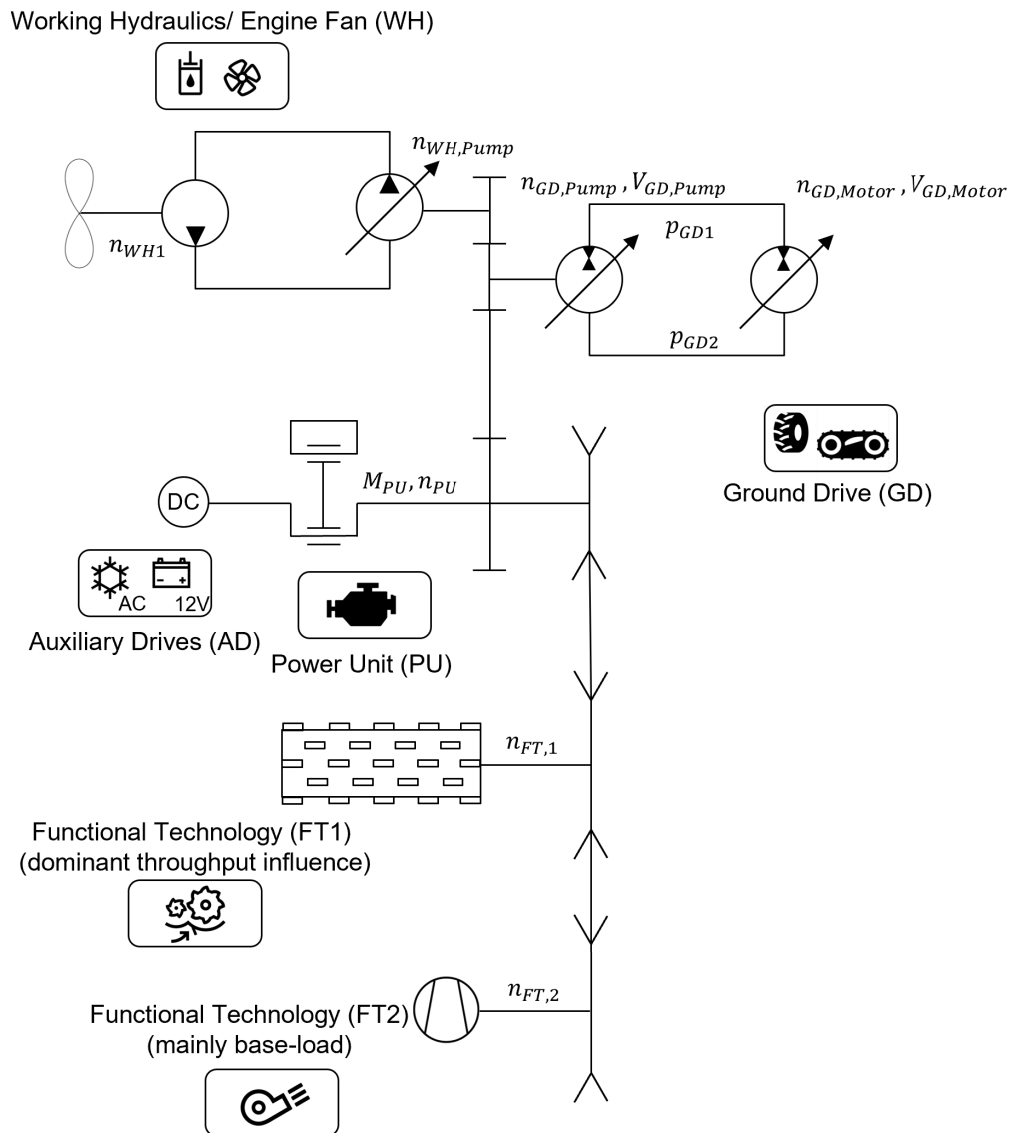


Figure 3: Schematic overview of the combine powertrain and the utilized data sources

Furthermore, this combine type is equipped with two throughput measurement devices. These consist of a facility to measure the overall throughput in the feeder house by a cross-section measurement of the straw mat, as well as a grain-based measurement of the resulting grain throughput in the elevator (Figure 4).

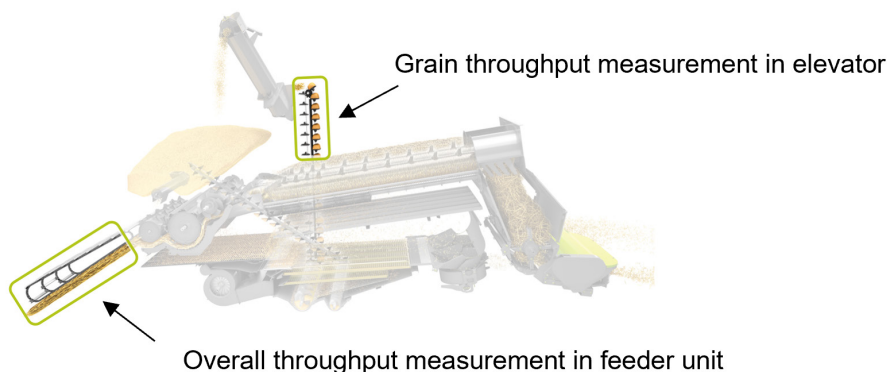


Figure 4: Location for measurements of machine throughput

With this setup, a measurement procedure is developed that allows the separated measurement of the three load types. Initially, the base load is recorded by an idle measurement consisting of a variation of adjustable aggregate speeds as well as switchable drives and couplings. This allows for modelling the load variance while stationary. In the second step, field measurements are performed that allow the determination of the traction- and throughput-induced loads.

With this recorded dataset, the information from the ground drive can be used to estimate the traction-induced losses on the pump and motor side of the hydrostatic unit. Thirdly, the throughput variation is used to achieve a measurement containing the process-induced load parts. Utilizing the prior base load measurement and the post-processed hydrostatic data of the ground drive pump, the throughput-induced torque can be estimated by a differential method. Therefore, the measured engine load is disassembled into the three introduced causal elements. Figure 5 shows a flowchart of the described procedure. Assuming the introduced superposition hypothesis, the data can then be recombined. This allows a simplified model representation of the measured machine data. In the following, the single measurement steps are explained in detail, illustrated by specific machine data.

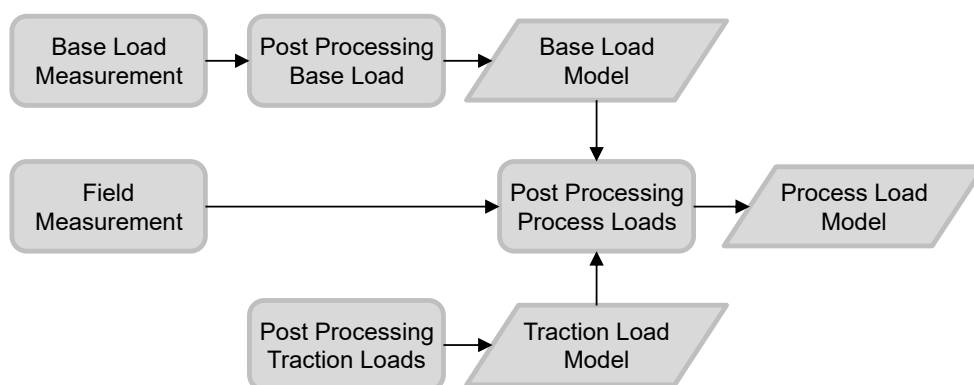


Figure 5: Flow chart of the proposed measurement procedure

Measurement and Modelling of Base Loads

Measuring the base loads of the combine is a first step of importance, as it already explains a significant share of the load as well as a significant degree of variability in load data. Following the introduced measurement concept, there is only a single measurement source of torque, making an estimation of absolute power flows of single individual components impossible. Instead, a differential

method is chosen, which represents the variability of the powertrain regarding adjustable machine parameters. This is sufficient for the modelling of existing machine concepts as it describes all achievable operation points exhaustively. To reach this goal, the occurring base loads are grouped into three categories:

- Constant base loads – without main drive
- Constant base loads – with main drive
- Variable loads

Figure 6 gives a graphical overview of the measurement procedure:

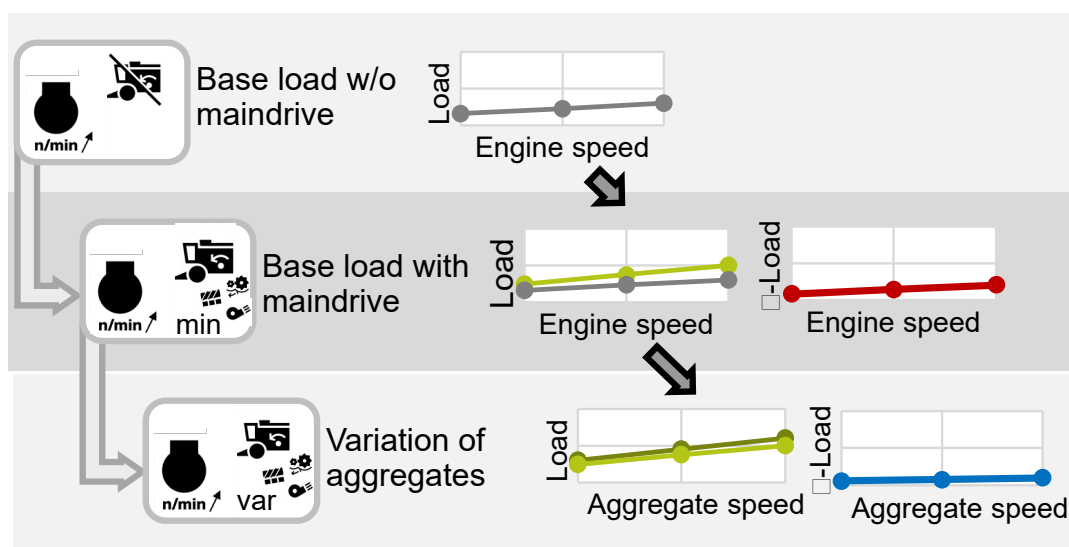


Figure 6: Concept for the base load measurement procedure

The measurement begins with estimating the constant base loads, which depend solely on engine speed and do not vary with transmission. Without the main drive engaged, these loads result from gearbox losses for the hydraulic units and auxiliary consumers on the engine side. A constantly driven engine fan, if installed, is included. The engine's drag torque is excluded as the torque balance is crankshaft-oriented. To measure the base load, the machine is warmed up with the main drive engaged to reach sufficient temperature. Starting from the lowest engine speed, a first base curve is recorded without the main drive. If a variable engine fan is installed, it is set to minimum. Next, the main drive, including the chopper unit and an attached header, is engaged. A second base curve is recorded by turning all aggregates to their minimum and then raising the engine speed in steps. By comparing both measurements, a differential curve is created by subtracting the base load without the main drive from the one with the main drive. This models the load effect of the main drive engagement and its connected base loads. Figure 7 shows the measurement of the base load and the additional load by engaging the main drive at high and low engine speeds of a LEXION 8000.

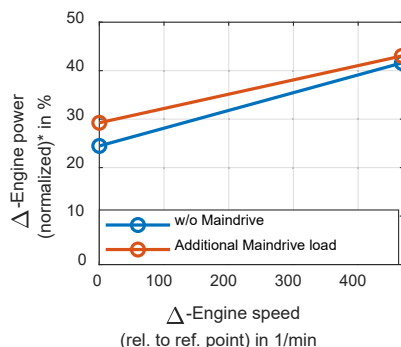


Figure 7: Base load and additional load through main drive, *normalized to idle (see Figure 13)

All values for the differential power are normalized to the idle power at high idle speed for the standard parameters of “wheat”. Subsequently, each tunable aggregate speed is varied (threshing drum, separator, cleaning fan, engine fan) while holding the others at minimum. Furthermore, the cutter bar and the chopper are disengaged as a variation. Again, difference lines from the variation measurement versus the base load with the main drive engaged can be calculated, allowing for modelling the variation of the single aggregates (Figure 8-12).

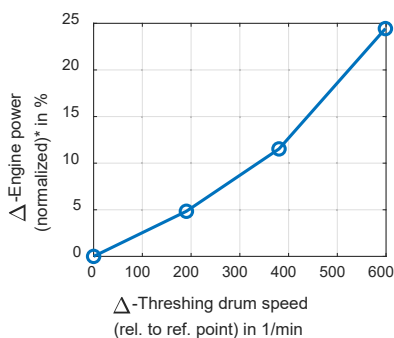


Figure 8: Relative influence of threshing drum on base load – *normalized to idle power

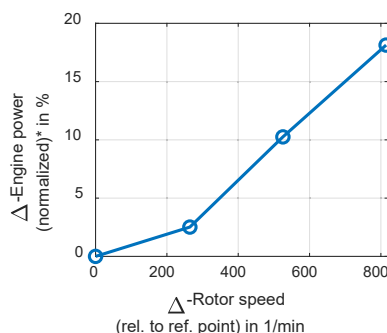


Figure 9: Relative influence of separation rotor on base load – *normalized to idle power

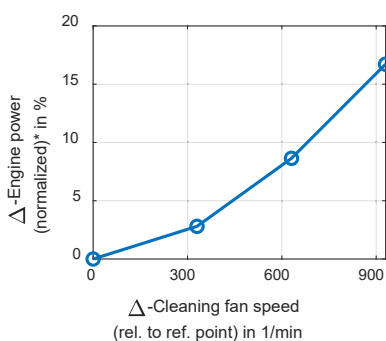


Figure 10: Relative influence of cleaning fan on base load – *normalized to idle power

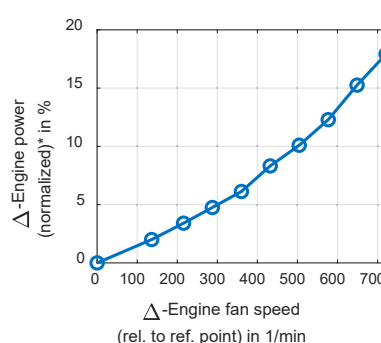


Figure 11: Relative influence of engine fan on base load – *normalized to idle power

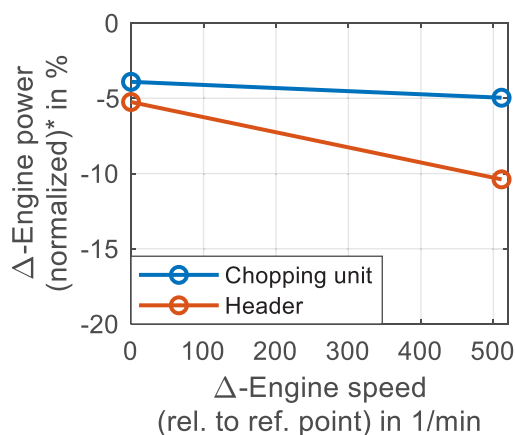


Figure 12: Power reduction through the disengagement of the chopper unit and the header – *normalized to idle power

Assuming a superposability of the single effects, all possible variations of the powertrain regarding the base load can be modelled. To illustrate the validity of the approach, the base load of a standard wheat configuration is calculated with the deduced differential curves. Then, this result is compared to measured loads (Figure 13). As can be seen, the simple linear superposition theorem shows sufficient accuracy. Still, if data and calculation capacity do not play a significant role, it is possible to measure factor combinations in a full factorial manner and model them by multidimensional interpolation.

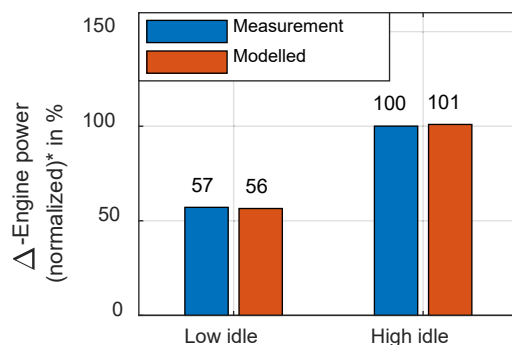


Figure 13: Exemplary comparison of idle loads – Machine in standard wheat configuration – measurement vs. superposed model values – *normalization point: measured idle-power at high-idle

Measurement and modelling of traction-induced loads

Traction-induced loads can be estimated using available information from the hydrostatic units. Therefore, the hydrostatic units are used as hydraulic torque sensors. HÄBERLE (2019) already showed the viability of this approach. The measurement setup is comparable to Häberle’s approach, using a torque balancing equation over the single units. By measuring the pressure before and after the units in combination with an estimation of the geometric displacement based on the solenoid amperage of the unit, the ideal hydraulic torque can be calculated. By correcting it using the supplier’s efficiency maps, it is possible to estimate the mechanical torque of the units (Equation 4).

$$M_{mech} = \frac{\eta_{hm}^w \cdot (p_1 - p_2) \cdot V_g}{2 \cdot \pi}$$

$$w = sig(p_1 - p_2) \cdot sig(n) \tag{Eq. 4}$$

$$\eta_{hm}^w = f(\Delta p, n)$$

with:

| | | |
|---|--|---------------------------------------|
| M_{mech} : Mechanical Torque at unit | V_g : Geometric displacement of unit | $p_1, \Delta p$: Pressures over unit |
| η_{hm} : Hydro-mechanical efficiency | n : Rotational speed of unit | w : Pump- or motor-operation (1/-1) |

Calculating the torque balance of the hydraulic motor over the axle transmission and assuming a dynamical wheel radius the wheel/track-forces can be estimated (Equation 5).

$$F_{Wheel} = \frac{M_{mech} \cdot i_{trans} \cdot \eta_{trans}}{r_{dyn}} \tag{Eq. 5}$$

with:

| | |
|--|---|
| F_{Wheel} : Mechanical force at wheel-contact | i_{trans} : Transmission ratio of the axle-transmission |
| M_{mech} : Mechanical torque at hydraulic unit | η_{trans} : Efficiency of the axle transmission |
| r_{dyn} : Dynamic rolling radius | |

Figure 14 and Figure 15 show an exemplary speed profile with the measured wheel forces from a machine with a rubber-belt drive in field operation under dry conditions on wheat-stubbed gley soil. The profile was measured in flat land conditions in Eastern Germany in August 2023. The stock conditions and the restrictions of the threshing process led to a speed of approximately 4 km/h during threshing. In the first headland, a three-point turn is shown. The other headlands are performed with 180-degree turning patterns with headland speeds peaking at over 10 km/h. At the end of the measurement, an unloading while standing is visible. Figure 16 and Figure 17 show an exemplary detailed view of one lane and adjacent headlands.

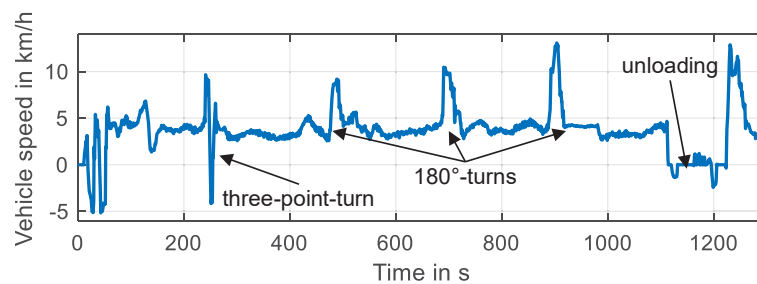


Figure 14: Exemplary vehicle-speed profile of a combine of the Claas Lexion 8800TT during threshing season 2023, dry gley-soil, machine with rubber tracks

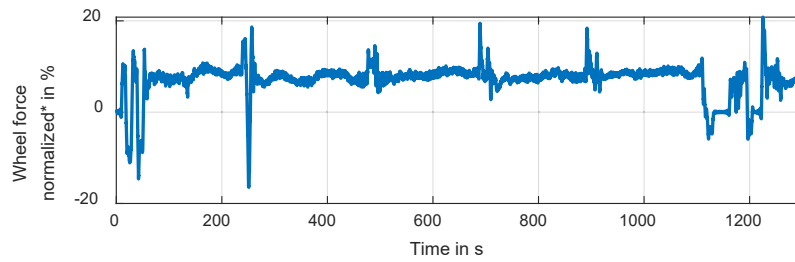


Figure 15: Illustration of the determined wheel force – *normalized to weight force of vehicle

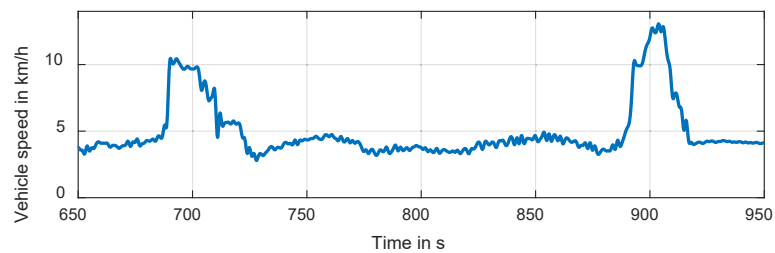


Figure 16: Exemplary detailed view of one lane with 2 adjacent headlands – vehicle speed

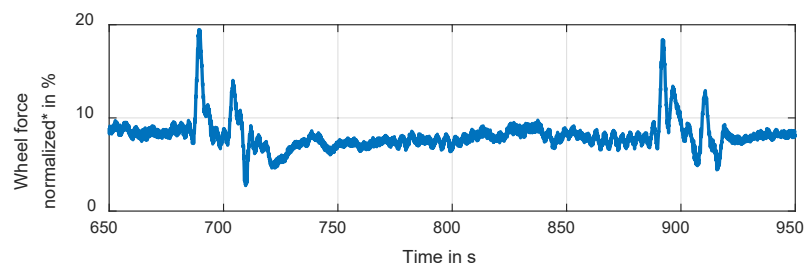


Figure 17: Exemplary detailed view of one lane with 2 adjacent headlands – *normalized to weight force of vehicle

Based on the provided wheel force, the driving resistance can be modelled. For agricultural machinery, the factor of slip on low-cohesion surfaces needs to be considered. For the correlation “slip/circumferential force,” common approaches with limited-growth characteristics are assumed (STEINKAMPF 1974, GRISSE et al. 2006, SCHREIBER 2006) which are based on empirical measurements of traction curves. These can be either implemented by measurement tables or by fitted algebraic expressions. Equation 6 shows an exemplary approach for that purpose (SCHREIBER 2006).

$$\mu = a_1 \cdot (1 - e^{-b_1 \cdot \sigma}) + c_1 \cdot \sigma \tag{Eq. 6}$$

with:

σ : Slip

a_1, b_1, c_1 : Regression factors

μ : Gross traction factor

In contrast to heavy tillage applications, common levels of slip are significantly lower in harvesters as the wheel forces are primarily needed to overcome rolling resistance and additionally to accelerate the machine. Figure 18 shows a normalized collective of circumferential forces for a LEXION 8800TT during threshing operations in wheat as an indicator for the general gross traction ratio and rolling resistance. The presented load collective results in comparatively low values for needed gross traction ratios, depending on the axle configuration and drive concept, and lies significantly below those of common traction-focused applications (RENIUS 2020).

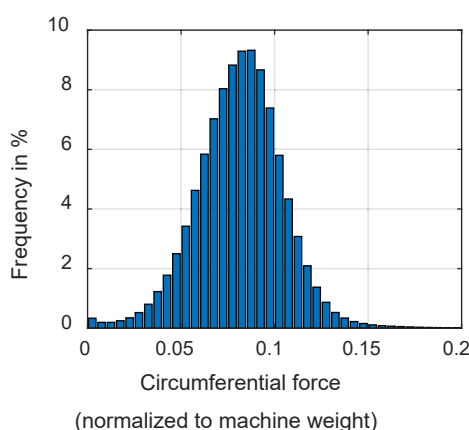


Figure 18: Exemplary distribution of circumferential forces on a CLAAS LEXION 8800TT during threshing operation in wheat (season 2023 - 74.8 h of operation time, dry gley soil, flat land)

Due to these low slip levels, it is challenging to collect data from specific field operations suitable for robust determination of traction characteristics, as it is not easily possible to measure the full traction bandwidth of a machine without an external source of drag force – however, it is also often not of special interest. For these reasons, it is proposed to use generalized slip/traction characteristics based on literature values for modelling purposes (STEINKAMPF 1974, GRISSE et al. 2006, SCHREIBER 2006), where the topic of traction does not play a significant role. If of special interest, it is possible to record the traction characteristics of the specific machine with additional equipment to apply a braking resistance in advance.

To formulate the driving resistance, the common approach of rolling resistance, slope force, and acceleration is chosen (Equation 1). Due to the low vehicle speeds and the predominant factor of high rolling resistance, the aspect of air resistance is neglected, leading to Equation 7.

$$m \cdot a = -m \cdot f_r \cdot g \cdot \cos(\alpha) - m \cdot g \cdot \sin(\alpha) + F_{wheel} \tag{Eq. 7}$$

With:

m : Vehicle mass
 a : Acceleration

f_r : Rolling resistance factor
 g : Gravity constant

α : Slope angle
 F_{wheel} : Wheel force

In this case, a simple speed-independent rolling resistance factor is assumed. If the modelling of a broader speed range is in focus, a speed-dependent modelling should be taken into consideration. Using the data of the vehicle acceleration from RTK-based GPS data and data from inclinometers (often already installed in series configuration on combines), the terms of acceleration and slope force can

be determined from the measurements. Subsequently, it is possible to estimate the rolling resistance by subtracting the acceleration and inclination force from the wheel force. The consideration of areas with constant speeds enhances the quality of the determined factor in this regard, as the acceleration as a possible error source can be reduced. Figure 19 shows an exemplary speed variation to determine the rolling resistance factor. Allocating the factor to a position vector, it is possible to create a field profile of the rolling resistance for modelling purposes. Doing so, the recorded traction-induced loads can be modelled in a position-based way, giving the opportunity to store information about load deviations in a position-based manner and to differentiate between rolling and slope resistance.

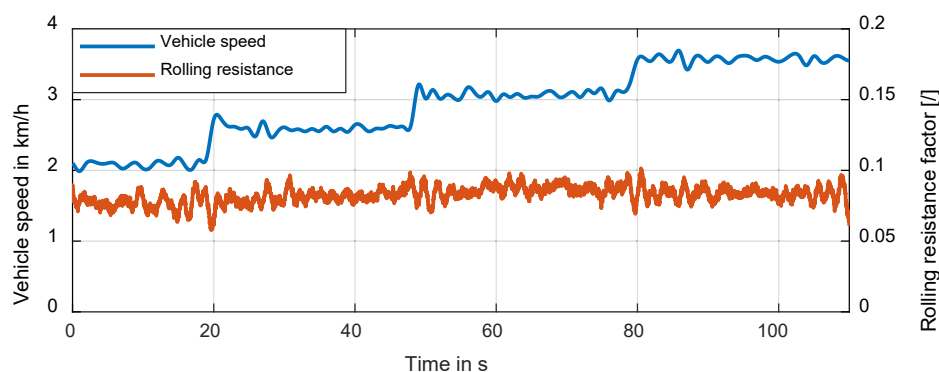


Figure 19: Exemplary determination of a constant rolling resistance factors on a speed step profile during harvesting at lower speeds

Modelling of process-induced loads

As a third step, it is necessary to describe the throughput-related loads. This needs to be performed as a subsequent step after estimating the traction-induced and base loads, as there is no separate measurement device for the process-induced loads. Rather, the base load and the traction-induced load are eliminated from the measured overall load to gain the process load profile. The traction-induced load can be estimated directly from the measurement on the level of the hydraulic ground drive pump, using the correlation from Equation 4. The base load is calculated using the model approach presented above. As a result, the remaining torque is allocated to the process being throughput-related. To achieve a reliable data basis, a throughput variation by holding different vehicle speeds in a stepped profile is performed. The main parameters of the functional technology (e.g., aggregate speeds, concave diameter, configuration of the chopper unit) influencing the process-specific power demand are kept constant. For illustration, an exemplary speed profile is shown in Figure 20 to Figure 23, including its resulting load share. Comparing Figure 20 and Figure 21, the expected linear correlation between speed and throughput can be observed. Still, the inhomogeneities in the yield and in the feeding process of the machine are clearly visible, leading to the variations of process-induced power visible in Figure 22 and Figure 23.

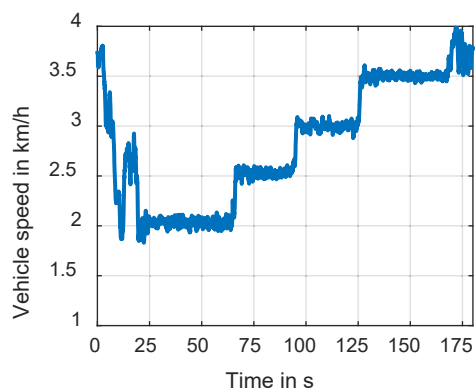


Figure 20: Profile of vehicle speed during throughput variation

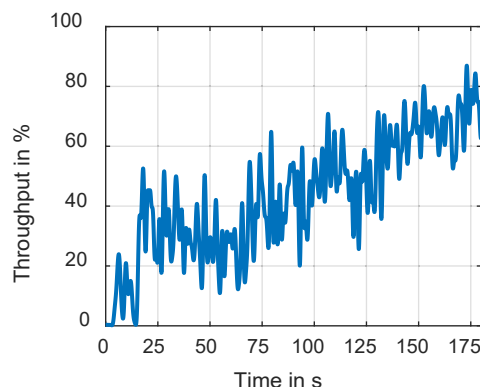


Figure 21: Throughput - measured in the feeder unit

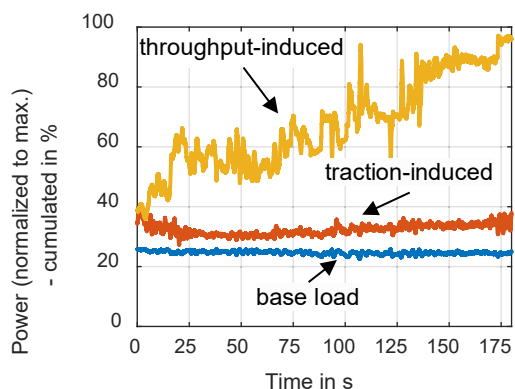


Figure 22: Cumulated machine load profiles with base load and traction-induced loads from previous determination steps

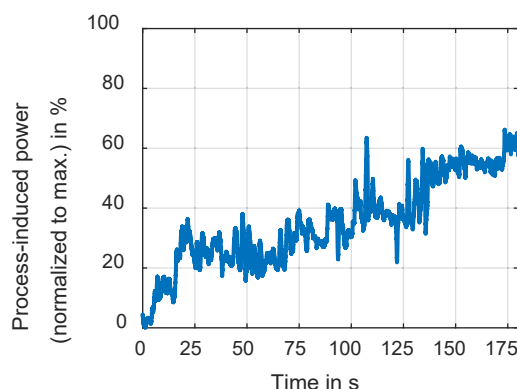


Figure 23: Resulting throughput-induced load - normalized to max. engine power

Analysing the resulting process-induced load, a plausible power distribution with a zero-load condition without throughput can be identified. To assess the correlation of the process-induced load and the throughput, a window-based post-processing filter algorithm is applied, which allows the determination of a threshing resistance. Therefore, a Savitzky-Golay filter of first order with a window length of 10 seconds is applied (Figure 24 and Figure 25). This smooths the dynamic build-up of torque induced by the sequence of power-consuming functional processes in the combine, leading to a signal representation of a more stationary process behaviour. After performing this filtering, a clear proportional trend between the throughput-induced load and the throughput can be identified, which fits the filtered profile values well (Figure 26 and Figure 27).

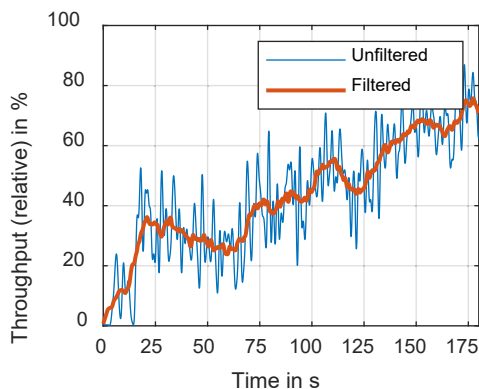


Figure 24: Smoothing the throughput profile by a Savitzky-Golay filter of first order (window-length: 10s)

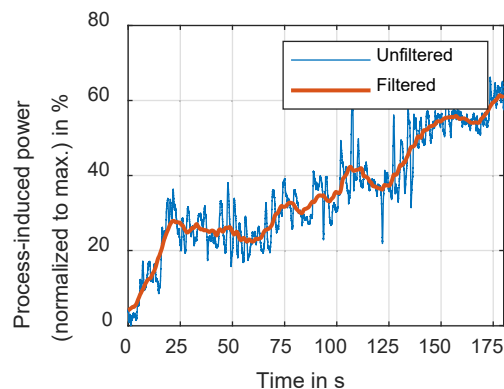


Figure 25: Smoothing the throughput-induced load profile by a Savitzky-Golay filter of first order (window-length: 10s) - normalized to max. engine power

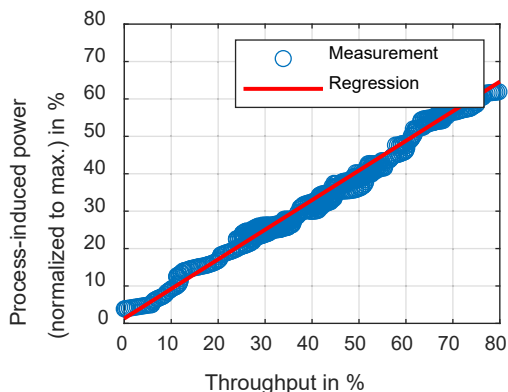


Figure 26: Proportional correlation between the process load and the throughput („threshing resistance“), normalized to maximum engine power

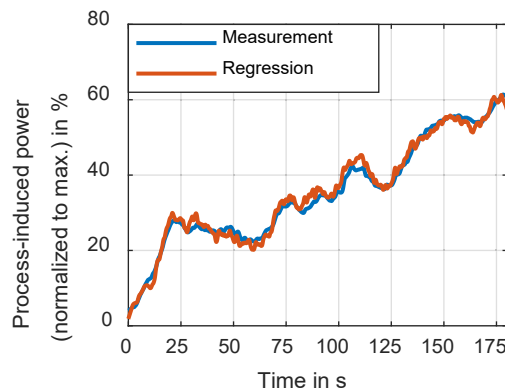


Figure 27: Profile of the dynamic accuracy of the linear regression, normalized to maximum engine power

By performing this filter-based analysis, the stationary crop-induced load dependence can be determined accordingly. However, due to the smoothing, significant characteristics of the dynamic process load behavior are not modelled accurately, demanding a more sophisticated approach for the assessment of load dynamics. For that purpose, a latency model with three elements, representing the three main power consumers of the throughput-affected functional technology (threshing system, separation, chopping unit), is introduced.

$$P_{process} = k_1 \cdot \dot{m}_{cpl}(t - T_1) + k_2 \cdot \dot{m}_{cpl}(t - T_2) + k_3 \cdot \dot{m}_{cpl}(t - T_3)$$

$$k_{cpl} = k_1 + k_2 + k_3 \tag{Eq. 8}$$

$$T_1 < T_2 < T_3$$

with:

\dot{m}_{cpl} : Throughput

t : Time

T_1, T_2, T_3 : Latencies

k_{cpl} : Threshing resistance

k_1, k_2, k_3 : Distribution of threshing resistance

By dividing the threshing resistance into three load partitions with different latencies, a dynamic model is created, which can subsequently be optimized to fit the measured process loads. This allows a realistic representation of the recorded loads, including dynamic effects. Table 1 and Figure 28 show the results for the fitted dynamic model. As can be seen, the loads as well as characteristic frequencies can be modelled accordingly. Expectedly, the result shows deviations regarding single occurring loads, which can be connected to inhomogeneities in the yield. Figure 29 gives an exemplary detail view to provide an impression of the dynamic quality. The range of occurring loads is represented sufficiently. Figure 30 and Figure 31 show the distribution of occurring loads as well as the main frequencies of the loads. It becomes visible that the main frequencies as well as the principal load distribution are captured by the model approach. Still, certain dynamics are not fully captured and remain a source of uncertainty. On one hand, the engine is operated in a speed-controlled manner, leading to potential load dynamics to accelerate the engine and transmission that are not modelled by the process-sided model approach. Therefore, a closed-loop representation would be needed. Furthermore, the factor of crop inhomogeneities and resulting effects (e.g., in the header and feeder house) are not modelled in their entirety. Still, the approach serves as an appropriate method to model principal load dynamics. With this approach, it is possible to depict a distinct configuration of engine and aggregate speeds. To illustrate the effect of different aggregate speeds, repeated measurements are needed.

Table 1: Optimized parameters for the dynamical process load model

| | | | |
|-----------|------|-------|--------|
| k_{cpl} | 0.79 | T_1 | 0.34 s |
| k_1 | 0.32 | T_2 | 1.09 s |
| k_2 | 0.27 | T_3 | 3.71 s |
| k_3 | 0.20 | | |

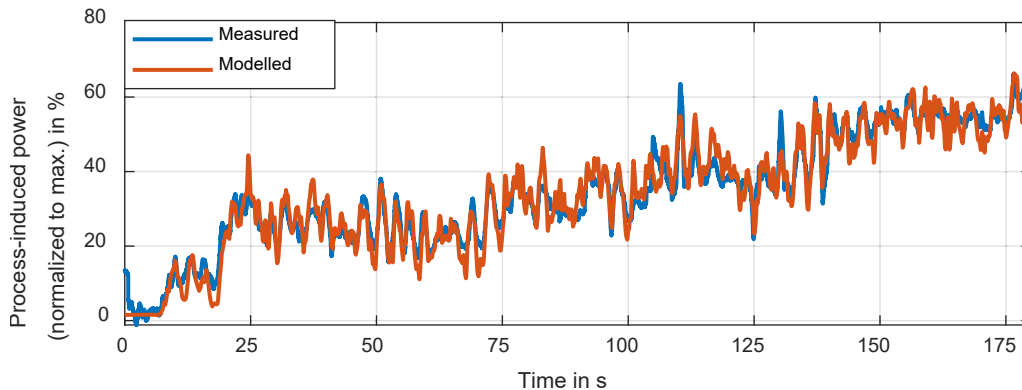


Figure 28: Application of the dynamical model to the speed step profile – normalized to max. engine power

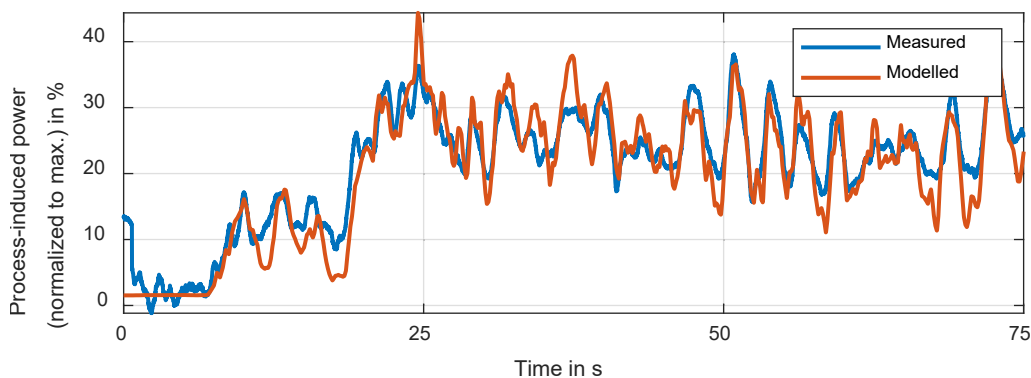


Figure 29: Application of the dynamical model to the speed step profile – exemplary detail view – normalized to max. engine power

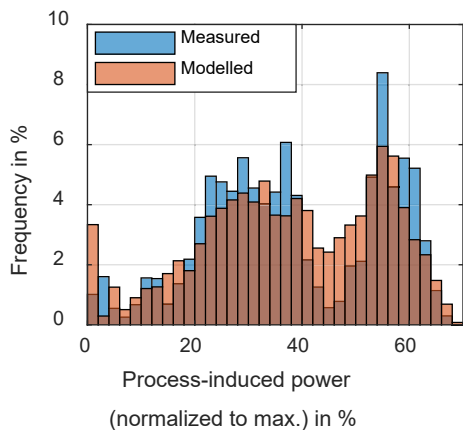


Figure 30: Distribution of loads – measured vs modelled – normalized to max. engine power

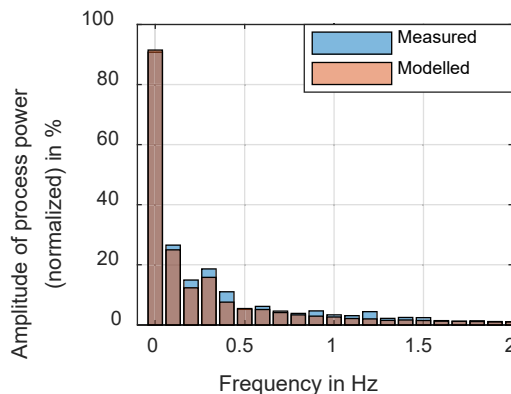


Figure 31: FFT-comparison of occurring load frequencies – measured vs modelled

Conclusions

Introducing principal concepts for lean modelling, a measurement and modelling approach for combine harvesting machinery is presented, which allows the representation of overall machine loads divided into three load categories: “base load,” “traction-induced load,” and “throughput-induced load.” In contrast to existing approaches, it does not model the power flows through the different branches of the powertrain in a source-based manner but allocates the loads to variable factors acting on the machine. By analysing existing measurement data as well as exemplary infield measurements, the validity of the approach and its transferability from existing data can be shown.

The method enables a lean measurement procedure to determine principal loads of combine powertrains without the necessity of extensive measurement equipment. Therefore, it can serve as a practical approach to model power requirements efficiently. The focus of the model lies not in the analysis of processes inside the functional systems of the machinery, but on the representation of measured loads depending on the dominant process factors. Overall machine loads can be modelled with a good coherence to the measured basis. Therefore, the approach can serve for subsequent comparisons of machine and powertrain efficiency as well as for interactive cycle generation. This allows, for example, the testing of different engine variants deviating in their maximal available power or a repeated optimization of control and design characteristics (e.g., vehicle-speed controls, definition of set-engine speeds) without the need for extensive in-field testing.

The next necessary step is the integration of these model approaches into a closed-loop environment, which allows the partly or fully virtual representation of a combine model. By introducing a divided process representation in the dynamic load model, it is furthermore possible to implement measurements and knowledge from source-based measurements of single aggregates into the process representation in future approaches. Therefore, more extensive measurement campaigns are needed to elaborate on the effect of single aggregate speeds on the process-induced loads.

This approach also allows the implementation of knowledge achieved by more extensive measurement campaigns and can close the gap between existing measurement approaches and the presented ones. In conclusion, the model approach transfers existing modelling knowledge of load phenomena in combine harvesting applications into a practicable format and can therefore be used for time-efficient analysis tasks of modern combine powertrains.

References

- Fillingham, R. (2017): Measuring and Modelling the Greenhouse Gas Emissions of a Combine Harvester. Dissertation, Harper Adams University
- Grisso, R.; Perumpral, J.; Zoz, F. (2006): An empirical model for tractive performance of rubber-tracks in agricultural soils. *Journal of Terramechanics* 43(2), S. 225–236, <https://doi.org/10.1016/j.jterra.2005.12.002>
- Häberle, S. (2019): Anforderungs- und einsetzungsgerechte Auslegung von Fahrtrieben mobiler Erntemaschinen. Dissertation, Universität Stuttgart
- HAWE Hydraulik SE (2023): Fluidlexikon - hydraulisch-mechanischer Wirkungsgrad. <https://www.hawe.com/de-de/fluidlexikon/hydraulisch-mechanischer-wirkungsgrad/>, accessed on 3 Feb 2024
- Küçükay, F. (2022): Grundlagen der Fahrzeugtechnik – Antriebe, Getriebe, Energieverbrauch, Bremsen, Fahrdynamik, Fahrkomfort. Wiesbaden, Springer Fachmedien Wiesbaden GmbH
- Meiners, A. (2023): Potentialbewertung effizienzsteigernder Technologien bei Landmaschinen in Verfahrensketten mit Körnerfruchternte. Dissertation, Universität Stuttgart

- Meiners, A.; Böttinger, S. (2018): Leistungsbedarf und Leistungsverteilung im Mähdrescher – Untersuchung zukünftiger Einsparpotenziale im realen und virtuellen Versuch. In: Land.Technik AgEng 2018, VDI Verlag, S. 149–157
- Müller, C.; Anderl, T.; Böttinger, S. (2012): Lastkollektive und Leistungsverteilung am Mähdrescher. Landtechnik 67(4), S. 270–273, <https://doi.org/10.15150/LT.2012.308>
- Renius, K. T. (2020): Fundamentals of Tractor Design. Cham, Springer International Publishing
- Rohrer, R.A.; Luck, J.D.; Pitla, S.K.; Hoy, R. (2018): Evaluation of the Accuracy of Machine Reported CAN Data for Engine Torque and Speed. Transactions of the ASABE 61(5), pp. 1547–1557, <https://doi.org/10.13031/trans.12754>
- Schreiber, M. (2006): Kraftstoffverbrauch beim Einsatz von Ackerschleppern im besonderen Hinblick auf CO₂-Emissionen. Dissertation, Universität Hohenheim
- Schwehn, J.; Ernst, V.; Böttinger, S. (2021): Eine praxisoptimierte Methodik zur Messung des Rollwiderstands von Traktorreifen. Landtechnik 76 (4), S. 142–155, <https://doi.org/10.15150/lt.2021.3271>
- Steinkampf, H. (1974): Ermittlung von Reifenkennlinien und Gerätezugleistungen für Ackerschlepper. Dissertation, Technische Universität Carolo-Wilhelmina zu Braunschweig
- Wohlfahrt, F.; Göres, T.; Terörde, S.; Frerichs, L. (2024): Standardized Short-Cycle Measurement Approach of Powertrain-Load-Scenarios for Combine Harvesting Machinery. agricultural engineering.eu 80(1), <https://doi.org/10.15150/ae.2025.3328>

Authors

Fabian Wohlfahrt, M.Sc., is a Development Engineer, **Dr.-Ing. Thomas Göres** is Vice President SF Advanced Development, **Dipl.-Ing. Stefan Terörde** is Head of Advanced Development Functional Technology at CLAAS Selbstfahrende Erntemaschinen GmbH, 33428 Harsewinkel. E-mail: Fabian.Wohlfahrt@claas.com

Prof. Dr. Ludger Frerichs is Head of the Institute of Mobile Machines and Commercial Vehicles, Technische Universität Braunschweig, 38106 Braunschweig.